Kinesin-1-mediated axonal transport of CB1 receptors is required for cannabinoid-dependent axonal growth and guidance

Trinidad M. M. Saez, Iván Fernandez Bessone, María S. Rodriguez, Matías Alloatti, María G. Otero, Lucas E. Cromberg, Victorio M. Pozo Devoto, Gonzalo Oubiña, Lucas Sosa, Mariano G. Buffone, Diego M. Gelman and Tomás L. Falzone
DOI: 10.1242/dev.184069

Editor: Paola Arlotta

Review timeline

Original submission:	21 August 2019
Editorial decision:	15 October 2019
First revision received:	22 January 2020
Accepted:	23 February 2020

Original submission

First decision letter

MS ID#: DEVELOP/2019/184069

MS TITLE: Kinesin-1-mediated axonal transport of CB1 receptors is required for cannabinoid-dependent axonal growth and guidance

AUTHORS: Trinidad M Saez, Matias Alloatti, Maria Gabriela Otero, Lucas Cromberg, Ivan Fernandez Bessone, Victorio Pozo Devoto, Maria sol Rodriguez, Gonzalo Oubina, Mariano G Buffone, Diego Gelman, and Tomas Falzone

I am sorry for the delay in sending this to you. I was waiting for the comments of a third reviewer, which in the end is taking way too long to get back to us. Given that there is agreement between the two current reviewers and that I also agree with them, I am sending you my answer at this point. The referees' comments are appended below, or you can access them online: please go to BenchPressand click on the 'Manuscripts with Decisions' queue in the Author Area.

As you will see, the referees express considerable interest in your work, but have some significant criticisms and recommend a substantial revision of your manuscript before we can consider publication. There is particular concern about the statistical analysis of the data and the need for additional in vivo validation. If you are able to revise the manuscript along the lines suggested, which may involve further experiments, I will be happy receive a revised version of the manuscript. Your revised paper will be re-reviewed by one or more of the original referees, and acceptance of your manuscript will depend on your addressing satisfactorily the reviewers' major concerns. Please also note that Development will normally permit only one round of major revision.

Please attend to all of the reviewers' comments and ensure that you clearly highlight all changes made in the revised manuscript. Please avoid using 'Tracked changes' in Word files as these are lost in PDF conversion. I should be grateful if you would also provide a point-by-point response detailing how you have dealt with the points raised by the reviewers in the 'Response to Reviewers' box. If you do not agree with any of their criticisms or suggestions please explain clearly why this is so.

Reviewer 1

Advance summary and potential significance to field

This study investigated the role of kinesin-1 in the axonal transport of the CB1 receptor, the key neuronal GPCR active at the endocannabinoid signaling and a key player in numerous processes of the neuronal development in humans and laboratory species. To this end, authors conducted a series of well-designed experiments with timely and useful experimental tools. Their results are interesting and, in general, support the findings described in the text.

Comments for the author

1. The major problem with this study is replicability, as authors used relatively small sample sizes in some experiments, for example n=3-4 in the data shown in Figure 1. In addition, the legends to Figures 3, 7, 8 and 9 should indicate not only the number of measures (growth cones, neurons, etc) but the number of experiments or subjects, which is the key element for ensuring replicability, as they did in Figure 6. This should be also indicated for the data in Figures 4 and 5. In my opinion, authors must consider the need more replications in some experiments.

2. Genetic rescue experiments with KLC1 would be of interest for some of the in vitro experiments conducted in this study, for example those included in the Figure 3.

3. Materials and Methods section should end with a description of the statistical methods used to assess the data.

4. Authors mentioned several times the words “recent studies” for publications that were not really recent. See examples in lines 70-72 (2015 is not recent), 81-85 (studies published in 2012-2016 are not recent), 321-323 (2016). This possibly responds to the fact that, in general, the list of references is not particularly updated in a field that is moving fastly in the last years. Only 10 articles of a total of 55 in the list were published after 2015, so less than 20%. The list needs to be updated with some recent studies of researchers active in this field, who generated important data that have not been mentioned despite is relevance for authors’ goals.

5. Somes typos: line 60: 2-arachidonoylglycerol; line 357: monoacylglycerol.

Reviewer 2

Advance summary and potential significance to field

Saez et al describe a neurodevelopmental defect of corticothalamic projection neurons in KLC1 mutant mice. They show that Kinesin-driven transport of CB1R is impaired in this mutant and that this leads to aberrant anterograde and retrograde transport and a phenotype in axon bundling, actin dynamics, and axonal elongation.

This paper is of interest for neurodevelopmental disorders and how axonal transport is involved in regulating signaling, such as growth cone guidance.

Comments for the author

Major points:

- Graphs are small and numbers hard to read.
- Figure 1: is there a way (electron microscopy?) to quantify the number of axons in KLC+/+ vs -/- mice or if axon caliber is changed?
- Figure 2: Is the tracing also possible for CFA axons? Is it possible to label single axon from CTA? This way, a sholl analysis would be helpful.
- Is it possible to perform time lapse imaging in embryonic slices to see outgrowth?
- Figure 3: I would highly recommend repeating the quantitative immunostaining of CB1R and L1- NCAM in single optical sections. Epifluorescence is not the

method of choice. Especially as the paper crucially depends on this. Why did the authors choose L1-NCAM? If there are axon bundles clustering differently, I would rather recommend a cytoskeletal marker instead.
- Figure 4B: misrouted axon bundles hard to see. Is it a pycnotic nucleus instead? At least a nuclear staining in addition or a single optical section is needed here.
- Why are the authors not coming back to CTA axons at all after Figure 1?
- Figure 5: a quantification in single optical section is needed here! How many vesicles colocalize with Kinesin?
- Figure 6: if flux of CBR1-GFP particles in anterograde and retrograde direction is similar, why are there CBR1 accumulations in the growth cone?
- Figure 6: Kinesin is specific for anterograde transport. Why is there also a significant reduction of transport in retrograde direction?
- Is the transport of CBR1-GFP altered when Kinesin is overexpressed?
- Time lapse imaging of growth cone to assess their dynamism in KLC-/- vs +/+ mice necessary.
- Kinesin is not a specific molecular motor. I recommend analyzing at least one more cargo to demonstrate how specific the overall finding is in these axons.
- Figure 9: a more detailed analysis is needed here. At least, a regular sholl analysis would help to support the conclusion that only axonal elongation is affected. How is the effect on axonal elongation fitting together with the changed axonal bundles in the beginning?
- Has the fasciculation defects something to do with membrane adhesion defects?

Statistics section is missing in Methods. Why did the authors use a t-test and not a non-parametric test? Are the data tested for normal distribution? Please state the number of experiments throughout the manuscript, not only the single axons.

Minor points:

- Figure 1: section thickness would help to better judge the phenotype.
- Line 128: Figure 1G does not exist.
- Line 140: “specific role”: I would tone this down a bit.
- Line 141: remove typos.
- Line 150: reference needed here!

First revision

Author response to reviewers' comments

Reviewer #1:

1. authors used relatively small sample sizes in some experiments, for example n=3-4 in the data shown in Figure 1. In addition, the legends to Figures 3, 7, 8 and 9 should indicate not only the number of measures (growth cones, neurons, etc) but the number of experiments or subjects, which is the key element for ensuring replicability, as they did in Figure 6. This should be also indicated for the data in Figures 4 and 5. In my opinion, authors must consider the need more replications in some experiments.

While the phenotypic results observed in the experiments are very strong, we agree with the reviewer on this observation and we have increased the statistical power of the results by including additional measurements in different Figures. We have set up new breedings to produce more animals and include them in the analysis of key parameters in different experiments. Specifically, we have increased from 4 to 8 the number of mice used to analyze the thickness of the internal capsule, the number of fascicles per area, and the diameter of individual fascicles after

L1-CAM staining. Also we have increased from 3 to 6 the number of mice used to analyze fascicle area. Therefore, new graphs that double the experimental number of mice are now presented and analyzed in Figure 1B, 1C, 1D and Figure 1F. Figure legends were also improved to include the n and the independent experiments generated. The number of mice analyzed in new Figure 4 was also increased to 5. In addition, new Figure 6 was re-done using Pearson colocalization analysis in confocal images.

Figure 1

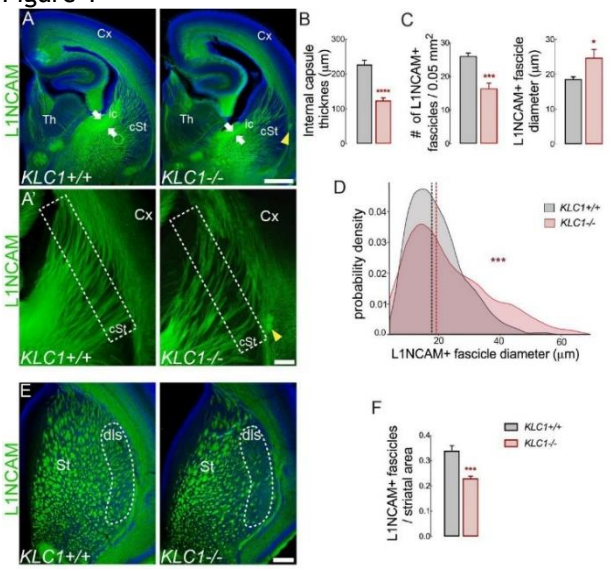

Figure 1. Axonal hyperfasciculation and pathfinding defects in *KLC1*$^{-/-}$ mice. (A) Representative epifluorescence images of 50 µm coronal brain sections (approximate position 255 in Allen Developing Mouse Brain Atlas) of L1-NCAM immunostaining counterstained with hoechst in *KLC1*$^{+/+}$ and *KLC1*$^{-/-}$ PD1 mice. White arrows indicate internal capsule thickness. Yellow arrows indicate ectopic axonal bundle in the corticostriatal boundary. (A') High magnifications of striatal fascicles. White rectangular boxes indicate representative areas quantified for axons in the caudal striatum. (B) Internal capsule thickness covered by L1-NCAM+ axons. Data is expressed as means ± s.e.m; *Student's t*-test; n = 8 animals / genotype from 3 independent experiments. (C) Number and diameter of individual L1-NCAM+ fascicles. Data is expressed as mean ± s.e.m. *Student's t*-test, n = 8 animals/genotype. (D) Probability density function analysis of fascicle diameter distribution between KLC1+/+ and KLC1-/- quantified in caudal striatum as shown in A'. *Kolmogorov-Smirnov* test. (n = 668 KLC1+/+, 362 KLC1-/- fascicles from 8 animals / genotype). (E) Representative epifluorescence images of 50 µm coronal brain section (approximate position 296 in Allen Developing Mouse Brain Atlas) of L1-NCAM immunostaining and hoechst in KLC1+/+ and KLC1-/- PD1 mice. Area enclosed in dashed line indicates dorsolateral striatum. (F) Striatal fascicles area relative to whole striatum area. Data is expressed as means ± s.e.m; *Student's t*-test, n = 8 animals / genotype. Abbreviations: cx, cerebral cortex; cSt, caudal striatum; dls, dorsolateral striatum; ic, internal capsule; st. striatum; th, thalamus. Scale bars: 500 µm (A); 100 µm (A', E). *p<0.025; **p<0.01; ***p<0.001.

2. Genetic rescue experiments with KLC1 would be of interest for some of the in vitro experiments conducted in this study, for example those included in the Figure 3.

Following the reviewer advice we have set up a rescue experiment in order to recover key phenotypes induced by KLC1 deletion. For this, we have set up the rescue of abnormal axonal transport of CB1R in KLC1-/- neurons. We are now showing that reduced transport properties of CB1R vesicles in KLC1-/- neurons are recovered with the overexpression of KLC1 motor protein. After transfecting *KLC1*-/- neurons with pcDNA-CB1R-EGFP (driving the expression of fluorescent CB1R) plus pcDNA-KLC1 (a vector driving the expression of KLC1) we observed a recovery of abnormal transport dynamics. In this condition, we have reverted to normal *KLC1*+/+ levels the transport properties of CB1R, which were impaired in *KLC1*-/-. This result, that is now immersed in new Figure 7, reinforce a key proposition of our work suggesting that KLC1 mediates the active axonal transport of CB1R vesicles. New Figure 7 is now as follow:

"To test whether CB1R transport defects were specifically induced by KLC1 deletion, we perform a rescue experiment by the overexpression of KLC1 in *KLC1*$^{-/-}$ neurons. Therefore, CB1R transport dynamics were analyzed after co-transfecting CB1R-eGFP plus pcDNA-KLC1 (a vector driving KLC1 expression) vectors in *KLC1*$^{-/-}$ neurons. Transfected neurons were stained with KLC1 antibody to confirm the recovery of KLC1 expression (Fig. 7B). The overexpression of KLC1 in neurons depleted of endogenous KLC1 restores the movement of CB1R vesicles by increasing anterograde and retrograde vesicle proportion to *KLC1*$^{-/-}$ levels and by reducing the proportion of stationary vesicles (Fig. 7D)."

Figure 7

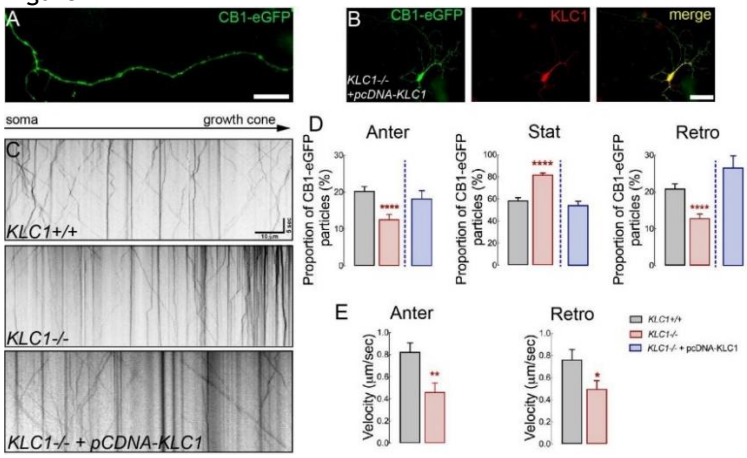

Figure 7. CB1R axonal transport is impaired in *KLC1*$^{-/-}$. (A) Representative epifluorescence images obtained from a live-cell movie of 7-8 DIV hippocampal neurons transfected with CB1R-eGFP. (B) Hippocampal neuron co-transfected with CB1R-eGFP plus pcDNA-KLC1 and immunostained for GFP and KLC1. (C) Kymographs of CB1R-eGFP transfected neurons obtained from live-cell imaging of *KLC1*$^{+/+}$, *KLC1*$^{-/-}$, and *KLC1*$^{-/-}$+pcDNA-KLC1 hippocampal cultures. (D) Anterograde, stationary and retrograde proportion of CB1R-eGFP vesicles, and (E) average velocities for anterograde and retrograde CB1R-eGFP vesicles. Data is expressed as means ± s.e.m. *Student's t*-test, n = 52 KLC1$^{+/+}$, 43 *KLC1*$^{-/-}$, 34 *KLC1*$^{-/-}$+pcDNA-KLC1 neurons from 3 independent experiments. Scale bar: 20 µm (A). **p<0.001, ***p<0.0001.

3. Materials and Methods section should end with a description of the statistical methods used to assess the data.

We apologize for the missing description of the statistical methods used. It is now included in materials and methods section and below. Figure legends are also now improved to show clearly the statistics used, n of experiments and significances.

"Statistical Analysis

Statistical differences between conditions were assessed using GraphPad Prism 8.2.1., MATLAB and R core team (2017). The normal distribution of the samples was assessed prior to analysis of significance. Values are expressed as means ± standard error of the mean (s.e.m.) or median ± 25/75 percentiles for non parametric data for the indicated number of independent experiments or corresponding particles (n). The experimental setting, the n, and the number of independent experiments are described in figure legends. No data was excluded from analysis. Images for analysis of intensity, quantification of axonal tracks from movies, or in Sholl analysis were double-coded so experimenter was blind to genotype or treatment. A two-tailed *Student's t*-test was used to compare differences between groups. Two-way ANOVA was performed to identify the interaction between two independent variables and analysis was followed by a *Bonferroni* post-test. *Kolmogorov-Smirnov* test was used to compare frequencies distributions of fascicles diameter, segmental velocities and axon diameters. Differences that resulted in $p < 0.05$ were considered to be significant."

4. Authors mentioned several times the words “recent studies” for publications that were not really recent. See examples in lines 70-72 (2015 is not recent), 81-85 (studies published in 2012-2016 are not recent), 321-323 (2016). This possibly responds to the fact that, in general, the list of references is not particularly updated in a field that is moving fastly in the last years. Only 10 articles of a total of 55 in the list were published after 2015, so less than 20%. The list needs to be updated with some recent studies of researchers active in this field, who generated important data that have not been mentioned despite is relevance for authors’ goals.

We acknowledge the point raised by the reviewer and we have updated our list of manuscripts to include the following citations:

Δ9-tetrahydrocannabinol and 2-AG decreases neurite outgrowth and differentially affects ERK1/2 and Akt signaling in hiPSC-derived cortical neurons. Shum C, Dutan L, Annuario E, Warre-Cornish K, Taylor SE, Taylor RD, Andreae LC, Buckley NJ, Price J, Bhattacharyya S, Srivastava DP. Mol Cell Neurosci. **2020**

Interference with the Cannabinoid Receptor CB1R Results in Miswiring of GnRH3 and AgRP1 Axons in Zebrafish Embryos. Zuccarini G, D'Atri I, Cottone E, Mackie K, Shainer I, Gothilf Y, Provero P, Bovolin P, Merlo GR. Int J Mol Sci. **2019**

Cell guidance ligands, receptors and complexes - orchestrating signalling in time and space. Rozbesky D, Jones EY. Curr Opin Struct Biol. **2019**

Understanding axon guidance: are we nearly there yet? Stoeckli ET. Development. **2018**

The F238L Point Mutation in the Cannabinoid Type 1 Receptor Enhances Basal Endocytosis via Lipid Rafts. Wickert M, Hildick KL, Baillie GL, Jelinek R, Aparisi Rey A, Monory K, Schneider M, Ross RA, Henley JM, Lutz B. Front Mol Neurosci. **2018**

Axonal transport: Driving synaptic function. Guedes-Dias P, Holzbaur ELF. Science. **2019**
Neuronal KIF5b deletion induces striatum-dependent locomotor impairments and defects in membrane presentation of dopamine D2 receptors. Cromberg LE, Saez TMM, Otero MG, Tomasella E, Alloatti M, Damianich A, Pozo Devoto V, Ferrario J, Gelman D, Rubinstein M, Falzone TL. J Neurochem. **2019**

Rapid assembly of presynaptic materials behind the growth cone in dopaminergic neurons is mediated by precise regulation of axonal transport. Lipton, D.M., Maeder, C.I., Shen, K. Cell Rep. **2019.**

The regulation of axon diameter: from axonal circumferential contractility to activity-dependent axon swelling. Costa AR, Pinto-Costa R, Sousa SC, Sousa MM. Front Mol Neurosci. **2018**

Prd1 associates with the clathrin adaptor α-Adaptin and the kinesin-3 Imac/Unc-104 to govern dendrite pruning in Drosophila. Zong W, Wang Y, Tang Q, Zhang H, Yu F. PLoS Biol. **2018**

Proteasome stress leads to APP axonal transport defects by promoting its amyloidogenic processing in lysosomes. Otero MG, Fernandez Bessone I, Hallberg AE, Cromberg LE, De Rossi MC, Saez TM, Levi V, Almenar-Queralt A, Falzone TL. J Cell Sci. **2018**

Mutation of Kinesin-6 Kif20b causes defects in cortical neuron polarization and morphogenesis. McNeely KC, Cupp TD, Little JN, Janisch KM, Shrestha A, Dwyer ND. Neural Dev. **2017**

Inputs from the thalamocortical system on axon pathfinding mechanisms. Garel S, López-Bendito G. Curr Opin Neurobiol. **2014**

5. Some typos: line 60: 2-arachidonoylglycerol; line 357: monoacylglycerol.

Typos were corrected and manuscript revised

Reviewer #2:

Graphs are small and numbers hard to read

All figures were now revised and modified to increase the size of graphs, labels and numbers so they should became easier to see in the final version

Figure 1: is there a way (electron microscopy?) to quantify the number of axons in KLC+/+ vs -/- mice or if axon caliber is changed?

This is a very interesting proposition that we have followed after the reviewer comment. We have now performed transmission electron microscopy (TEM) imaging to quantify the number and diameter of axons within the caudal striatum fascicles of PD1 mice. Interestingly, we have again confirmed by electron microscopy that fascicles in KLC1-/- mice are bigger. However, they did not show axon clustering, as previously thought, since the number of axons within fascicles were significantly reduced in KLC1-/- despite fascicles are bigger in total area. An extensive quantification using high resolution imaging by TEM showed that axon diameter within KLC1-/- fascicles are significantly enlarged. Together, these results revealed further insights on the defects induced by KLC1 deletion and are now included as new Figure 2. TEM images of fascicles and magnification of axons within fascicles are shown together with the quantification of average fascicle area, number of axons per area (30 μm^2), and frequency distribution of axon diameters. Interestingly, KLC1-/- fascicles showed a significant reduction in the number of axons. These additional experiments allowed us to further propose that during development of striatum axonal tracks in KLC1-/-, fewer axons reach the striatum fascicles, maybe because they are misrouted before crossing the striatal boundary due to pathfinding defects. In addition, the caliber of axons that forms the striatal fascicles in KLC1-/- are enlarged. TEM results are now included in new Figure 2 as follow:

“Fewer number but larger fascicle sizes in KLC1-/- suggests that striatum axon pathfinding is impaired.

To understand whether deletion of KLC1 induced axons to coalesce or to become dystrophic within abnormal fascicles we performed transmission electron microscopy (TEM) images from the caudal striatum in KLC1+/+ and KLC1-/- mice. The quantification of fascicle area by TEM again revealed enlarged fascicles in KLC1-/- compared with KLC1+/+ (Fig. 2A, B). We then performed high resolution TEM images to quantify the number and diameter of axons within the fascicles (Fig 2A’). Axon density and caliber was determined by manually counting and measuring axons in equal- sized boxes placed within the fascicles. Interestingly, we found a significant reduction in the number of axons per area in KLC1-/- compared with KLC1+/+ (Fig. 2C). However, the frequency distribution of axon diameter revealed that KLC1-/- presented a significant amount of enlarged or dystrophic axons (Fig. 2D). Together, these experiments suggest that fewer axons reach the striatum fascicles due to pathfinding defects and there is a significant dystrophic phenotype in KLC1-/- striatal fascicles.”

Figure 2

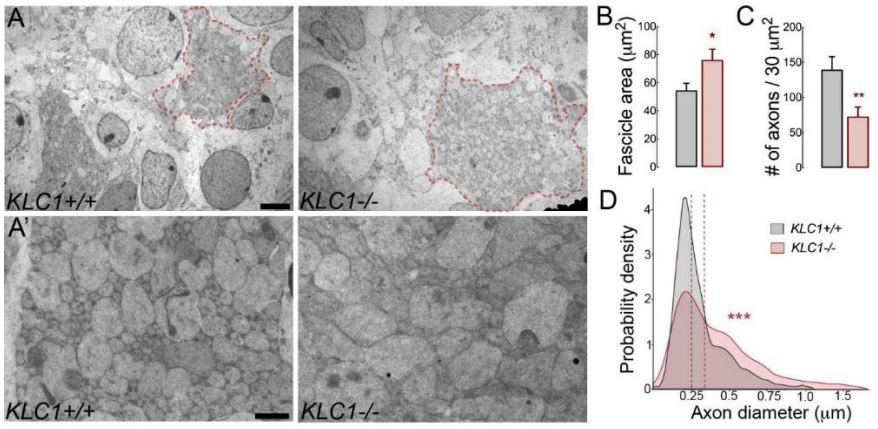

Figure 2. KLC1-/- display enlarged caliber but less axon number in abnormal striatal fascicles.

(A) Representative transmission electron microscopy (TEM) images showing axonal fascicles (dotted line) from caudal striatum in KLC1+/+ and KLC1-/- PD1 mice. (A') Higher TEM magnification images used to measure axonal diameters within fascicles. (B) Quantification of average fascicle area. Data is expressed as means ± s.e.m; *Student's t*-test, n = 11 KLC1+/+ and 14 KLC1-/- fascicles. (C) Average axon number per 30 μm^2 of fascicles. Data is expressed as means ± s.e.m; *Student's t*- test, n = 12 KLC1+/+ and 12 KLC1-/- fascicles (D) Probability density function analysis of pooled axon diameters between KLC1+/+ and KLC1-/-. *Kolmogorov-Smirnov* test. n = 1536 KLC1+/+ and 750 KLC1-/-. Scale bars: 2 μm (A), 0,5 μm (A'). *p<0.03; **p<0.01, ***p<0,001.

- Figure 2: Is the tracing also possible for CFA axons? Is it possible to label single axon from CTA? This way, a sholl analysis would be helpful.
As shown previously, DiI tracing was performed placing small amount of tracer in the primary somatosensory cortex to visualize Cortico-Fugal Axons (CFA) which include the Cortico-Thalamic xons (CTA). As we assumed, the reviewer suggested the reciprocal staining, that is, the Thalamo-Cortical Axons (TCA). Therefore, we have now performed new tracing experiments with DiI placed in the thalamic region after fixing PD1 mice and cutting the brain diagonally from inside. Therefore, we have now stained TCA that project to the cortex. Again, ***KLC1***-/- mice revealed a significant reduction of the internal capsule thickness, less dye reaching the cortical layers and also misrouted axons at the level of the cortical boundary. These results reinforce the proposition that both CTA and TCA, which depend on endocannabinoids signaling for proper development, are severely impaired. In addition, we are also including images from ***KLC1***-/- brain slices stained with CB1R antibody to clearly show the lack of CB1R positive axons reaching the thalamus (Figure 4, A''). The identification of single neurons to analyze the arborization was not feasible with DiI. However, a Sholl analysis was performed in neurons in culture treated with DMSO or ACEA. This analysis revealed that dendritic and axonal arborization in ***KLC1***+/+ and ***KLC1***-/- was similar, and no changes were induced by stimulation of CB1Rs with ACEA (Figure 10). These new experiments are now included in Figure 3 and 10, and the following was included in text:

"To test whether the lack of reciprocal connections also impair TCA we perform DiI experiment placing the dye at the thalamus after sectioning the brain diagonally from the midline (Fig. 3E). Interestingly, we found that ***KLC1***$^{-/-}$ present similar reductions in the internal capsule thickness (Fig. 3F, H), and also display misrouted axons at the level of the cortical boundary (Fig. 3G, arrow) that resulted in less DiI staining reaching the cortical layers (Fig 3F, arrow). Altogether, our results suggested that KLC1 might be involved in the development of CTA and TCA reciprocal connections. Interestingly, the abnormal fasciculation and misrouted axon phenotype is reminiscent to the defects observed in CB1R knock-out mice (Wu et al., 2010)."

FIGURE 3

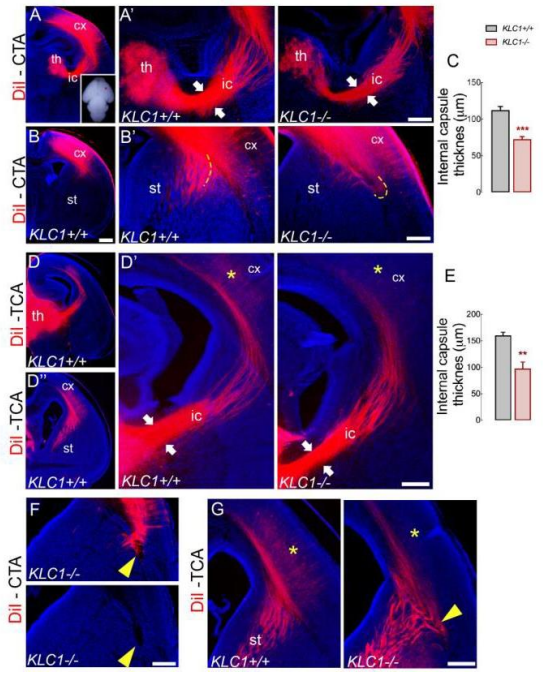

Figure 3. Reciprocal connection between the cortex and the thalamus is impaired in *KLC1*$^{-/-}$ mice. (A) Representative epifluorescence images of 100 µm coronal brain sections (approximate position 255 in Allen Developing Mouse Brain Atlas) after axonal tracing experiment with a carbocyanine dye DiI placed into the primary somatosensory cortex in PD1 mice (inset). DiI labeled CTA cross the internal capsule to reach the thalamus. (A') Higher-magnification images of *KLC1*$^{+/+}$ and *KLC1*$^{-/-}$ mice. White arrows indicate internal capsule thickness. (B) Rostral representative epifluorescence image of 100 µm coronal brain sections (approximate position 296 in Allen Developing Mouse Brain Atlas) after DiI tracing. (B') Higher-magnification images of *KLC1*$^{+/+}$ and *KLC1*$^{-/-}$ mice. White dashed line represent corticostriatal boundary. (C) Internal capsule thickness quantified after DiI labeled CTA. Data is expressed as means ± s.e.m; *Student's t*-test, n = 5 animals / genotype. (D) Ectopic CTA are observed in *KLC1*$^{-/-}$ mice. (E) Axonal tracing experiment with DiI placed into the Thalamus in PD1 mice. DiI labeled TCA cross the internal capsule to reach the cortex.

(F) Higher-magnification images of *KLC1*$^{+/+}$ and *KLC1*$^{-/-}$ mice. White arrow indicates internal capsule thickness. (G) Ectopic TCA are observed in *KLC1*$^{-/-}$ mice, yellow arrow. (H) Internal capsule thickness quantified after DiI labeled TCA. Data is expressed as means ± s.e.m; *Student's t*-test, n = 4 animals / genotype. Abbreviations: cx, cerebral cortex; ic, internal capsule; st. striatum; th, thalamus. Scale bar: 500 µm (A, C); 200 µm (A', C', D). **p<0.01, ***p<0,001.

- Is it possible to perform time lapse imaging in embryonic slices to see outgrowth?

This is a very nice experiment proposed by the reviewer; however, due to the necessary technical expertise and the methodological requirements, that we did not have running in the laboratory, we were unable to perform it in this revision time frame. We have tried to find collaborators that were available to help us on doing these experiments without success, however, we found the possibility to be trained in *in-utero* electroporation and we are in the process of acquiring an electroporator machine in the near future to perform this type of experiment. The plan will be to pursue this further and include new techniques in our laboratory.

- Figure 3: I would highly recommend repeating the quantitative immunostaining of CB1R and L1-NCAM in single optical sections. Epifluorescence is not the method of choice. Especially as the paper crucially depends on this. Why did the authors choose L1-NCAM? If there are axon bundles clustering differently, I would rather recommend a cytoskeletal marker instead.

As the reviewer suggested, we have now repeated the quantification performed in new Figure 4A, B in 0,2 µm-thickness single section images obtained in a Spinning Disk confocal microscope. As previously shown, we obtained now similar results showing a reduction of CB1R fluorescence intensity in *KLC1-/-* axons. In addition we quantified the fluorescence intensity of CB1R relative to L1NCAM in the axons that reach the thalamus, a region next to the internal capsule. Interestingly, we observed a reduction of 84% of CB1R levels in those axons in *KLC1-/- (Fig 4. A'', C)*. New Figure 4 is presented bellow. We have used L1-NCAM as it is highly enriched in axons during development; it clearly stains the axonal tracks from corticofugal and thalamocortical projecting neurons, and is widely used in bibliography. We followed the recommendation of the reviewer and we tested the neuronal b3-tubulin (TUJ1) staining as a cytoskeletal marker. We observed similar axonal staining with both antibodies, however, the staining with b3-Tubulin was more diffuse and axons harder to be observed compared with L1-NCAM. We include here a comparison of the staining that confirms a similar axonal staining with both antibodies, but after this preliminary result we stick to L1-NCAM staining in this experiment since gave a better result in our hands. New figure 4 is as follow:

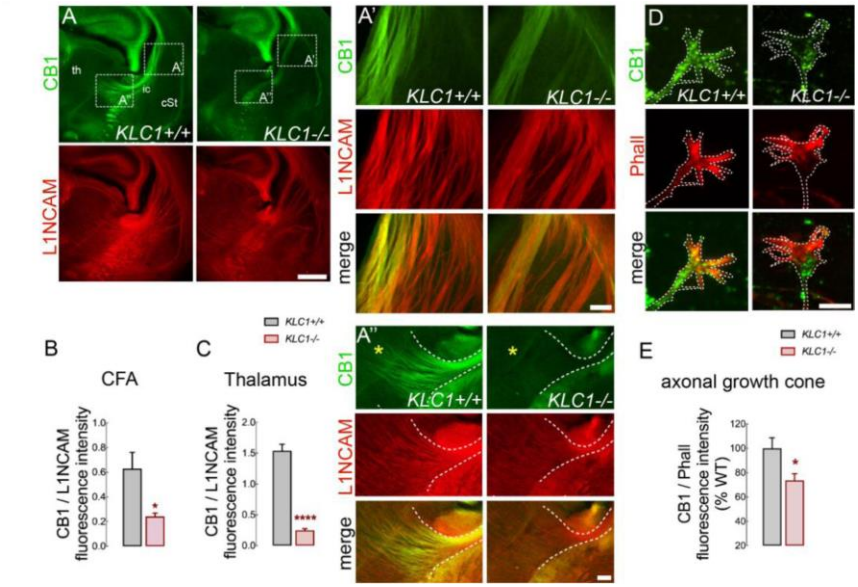

Figure 4. Reduced CB1R levels in axons and growth cones of *KLC1*$^{-/-}$. (A) Representative confocal images of coronal brain sections (approximate position 296, Allen Developing Mouse Brain Atlas) of L1-NCAM and CB1R immunostaining in *KLC1*$^{+/+}$ and *KLC1*$^{-/-}$ PD1 mice. White rectangular boxes located in the caudal striatum proximal to the (A') and thalamic region next to de internal capsule (A'') showing the area covered by CTA and TCAs used for quantification. (A', A") High magnification confocal images indicated in A. (B, C) Fluorescence intensity ratio of CB1R / L1-NCAM-positive fascicles quantified in *KLC1*$^{+/+}$ and *KLC1*$^{-/-}$ PD1 mice. Data is expressed as means ± s.e.m; *Student's t*-test, n = 3-4 sections per animal from 4 *KLC1*$^{+/+}$ and 5 *KLC1*$^{-/-}$ mice. (D) Representative high-resolution Spinning Disk Confocal Microscopy image of primary culture of CB1R and Phalloidin immunostaining in *KLC1*$^{+/+}$ and *KLC1*$^{-/-}$ axonal growth cone. (E) Quantification of fluorescence intensity ratio of CB1R / phalloidin relative to *KLC1*$^{+/+}$. Data is expressed as means ± s.e.m; *Student's t*-test, n = 60-70 growth cones / genotype from 2 independent experiments. Abbreviations: cx, cerebral cortex; ic, internal capsule; th, thalamus. Scale bar: 500 µm (A); 100 µm (A', A''), 20 µm (D). *p<0.01, ****p<0.0001.

Figure showing L1-NCAM and b3Tubulin staining.

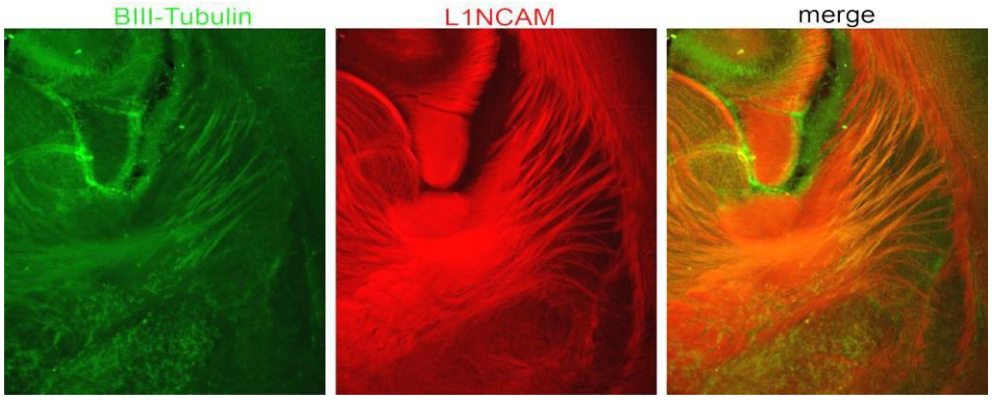

- Figure 4B: misrouted axon bundles hard to see. Is it a pycnotic nucleus instead? At least a nuclear staining in addition or a single optical section is needed here.

We have enlarged the image and included now the nuclear staining (Hoechst) in new Figure 5B to clearly show that this cluster corresponds to misrouted axons that accumulate before the striatum boundary.

Figure 5

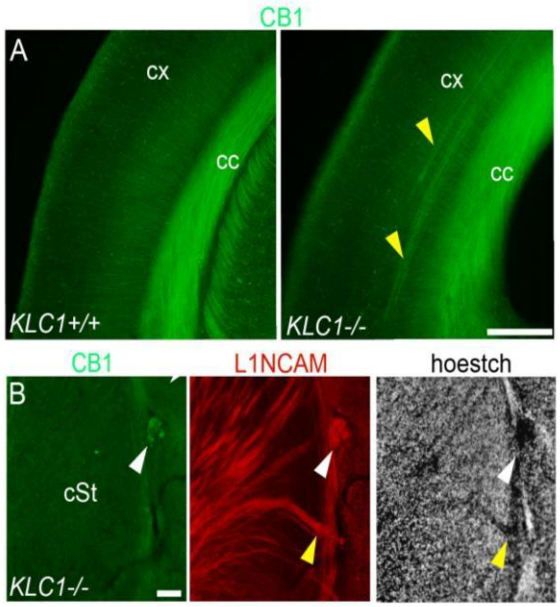

Figure 5. Misrouted axons in *KLC1*$^{-/-}$ brain are positive for CB1R. (A) Representative epifluorescence images of cerebral cortex immunostained for CB1R in *KLC1*$^{+/+}$ and *KLC1*$^{-/-}$ PD1 mice. Yellow arrows indicate ectopic cortical axon bundles positive for CB1R. (B) Magnification of the corticostriatal boundary immunostained for CB1R, L1-NCAM and Hoechst in *KLC1*$^{-/-}$ PD1 mice. White arrow indicates misrouted axon bundles devoid of nuclear staining. Abbreviations: cx, cerebral cortex; cc, corpus callosum. Scale bar: 200 µm (A), 50 µm (B).

- Why are the authors not coming back to CTA axons at all after Figure 1?
We apologize with the reviewer for not being clear in stating the type of neurons used in different Figures, and this is now corrected. We have performed many experiments in CFA after Figure 1. Previous experiments presented now in new Figure 3 were concentrated in tracing CTA axons with DiI placed in the primary somatosensory cortex. In addition, we have now included the reciprocal staining of TCA axons by placing DiI in the thalamus included as new Figure 3E, G. Again, results presented now in Figure 4A, B correspond to *in vivo* experiment focused on axons that initiate in the cortex from corticofugal neurons including the CTA and focusing on thalamic projections. In addition, new Figure 2 using TEM is focused on caudal striatal fascicles that include CTA. Figure 4 A, B include CTA axon staining. To understand the intrinsic cellular defects we have performed cortical neuronal cultures to observe their growth cones or axons in Figure 4C, D and Figure 5. Moreover, the analysis performed in Figure 8A, B involving the analysis of growth cones also correspond to cortical neurons in culture, and also in Figure 9 related to the extension of axons and where branching and Scholl analysis is now included,. We have now stated this in Figure legends and in text to make it easier to see.

- Figure 5: a quantification in single optical section is needed here! How many vesicles colocalize with Kinesin?

We have performed additional experiments in *KLC1*$^{+/+}$ cortical neurons to stain with antibodies against CB1R and kinesin heavy chain (KHC) after saponin treatment. We have performed spinning disk confocal imaging with 0,2 µm optical section and perform a Pearson correlation coefficient to quantify the degree of colocalization between fluorophores in 14 axons from *KLC1*$^{+/+}$ neurons. This result revealed a moderate degree of colocalization between CB1R vesicles and KHC. The result is now included as follow in text:

“To test whether Kinesin-1 may interact with CB1R vesicles to promote its axonal transport, we performed double-immunofluorescence staining for endogenous CB1R and the heavy chain subunits of kinesin-1 (KIF5) in saponin treated cortical neurons in culture before fixation in *KLC1*$^{+/+}$ (Fig. 6A). Single optical section of high resolution confocal images showed that CB1R vesicles partially co-

localized with KIF5s (KHC) in axons (Fig. 6A). Co-localizations were also evident at growth cones, where both CB1R and KHC accumulate. A Pearson quantification analysis revealed a moderate degree of colocalization (median 0,48, percentiles 25/75 = 0,367/ 0,545) between CB1R vesicles and KHC-positive vesicles in axons (Fig. 6B), suggesting the possibility that Kinesin-1 associates with CB1R containing vesicles and mediate their transport.

Figure 6

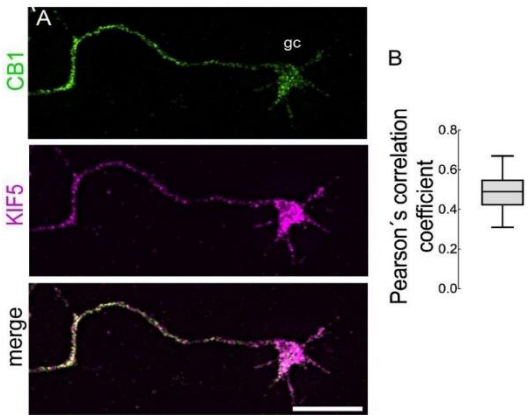

Figure 6. CB1R vesicles colocalize with Kinesin Heavy Chain subunits. (A) Representative high-resolution spinning disk confocal microscopy images of cortical neurons immunostained for endogenous CB1R and KHC. Merged image show CB1R and KIF5 colocalizing in vesicles from axons and growth cones (gc). (B) Quantification of colocalization between CB1R and KHC using Pearson's correlation coefficient. Data is expressed as median ± percentiles 25/75. n = 14 neurons. Scale bar: 10 µm.

- Figure 6: if flux of CBR1-GFP particles in anterograde and retrograde direction is similar, why are there CBR1 accumulations in the growth cone?

As the reviewer pointed out, there is no significant vias in the proportion of anterograde to retrograde vesicle direction that justify the accumulation of CB1R at growth cones as we have observed previously for other cargos. However, a steady state level at an end point of transport, such as, the growth cone is considered a place where vesicles can be directed to accumulate due to plasma membrane presentation or internalization processes. Moreover, intracellular dynamics of particles depends on many different and complex parameters that go beyond the proportion of vesicle movement. Therefore, even with similar proportions of anterograde to retrograde movement of vesicles, the average speed of movement that is composed of many types of segmental velocities can contribute to a preference displacement of vesicles. In the case of CB1R axonal transport, we have observed slight but consistent increases in anterograde run length. Moreover, anterograde segmental velocities distribution showed increased frequencies of faster speeds and reduced frequencies of slower speeds compared with the distribution of retrograde segmental velocities. Together, runs and segmental velocities influence the flux toward the synapse that poses a steady state accumulation of CB1R vesicles. The highly balanced transport for CB1R might be associated with changes in CB1R distribution between development and adult neurons that go from axonally enriched during development to presynaptic enriched in adult neurons.

Figure 6: Kinesin is specific for anterograde transport. Why is there also a significant reduction of transport in retrograde direction?

Vesicular cargos that moves in the axon in both anterograde and retrograde direction have been proposed to perform this type of movement due to the coordinated assembly of both anterograde (kinesin) and retrograde (dynein) motors. This coordination has been also suggested since there is direct interaction between proteins of the dynein complex and adaptor proteins for kinesin motors. Therefore, it is suggested that kinesin-1 motor can also mediate dynein recruitment to the cargo. Reduction of kinesin can lead to a reduced number of active dynein in a cargo and therefore not

only impair the anterograde transport but also the retrograde movement. We have included this interpretation in discussion as follow:

“A coordinated-competition model has been proposed to take place during axonal transport regulation of fast moving vesicles (Lacovich et al., 2017). In agreement with this model the deletion of *KLC1*, a subunit of the anterograde motor Kinesin-1, induced defects in both anterograde and retrograde, proportions, segmental velocities and run lengths. A possible explanation for the changes in CB1R retrograde movement when an anterograde motor is missing is supported by the kinesin-1 dependent recruitment of the dynein retrograde complex to the cargo, as it was shown for other vesicles (Szpankowski et al., 2012; Twelvetrees et al., 2016).”

- Is the transport of CBR1-GFP altered when Kinesin is overexpressed?

We are now showing the recovery of impaired axonal transport of CB1R in *KLC1*-/- neurons. For this, we have set up the rescue of abnormal axonal transport of CB1R in *KLC1*-/- neurons. We are now showing that reduced transport properties of CB1R vesicles in *KLC1*-/- neurons are recovered with the overexpression of KLC1 motor protein. After transfecting *KLC1*-/- neurons with pcDNA-CB1R-EGFP (driving the expression of fluorescent CB1R) plus pcDNA-KLC1-TAP-TAG (a vector driving the overexpression of KLC1) we observed a recovery of abnormal transport dynamics. In this condition, we have reverted to normal *KLC1*+/+ levels the transport properties of CB1R, which were impaired in KO. This result, that is now immersed in new Figure 7, reinforce the proposition of our work suggesting that KLC1 mediates the active axonal transport of CB1R vesicles. New Figure 7 is now as follow:

“To test whether CB1R transport defects were specifically induced by KLC1 deletion, we perform a rescue experiment by the overexpression of KLC1 in *KLC1*$^{-/-}$ neurons. Therefore, CB1R transport dynamics were analyzed after co-transfecting CB1R-eGFP plus pcDNA-KLC1 (a vector driving KLC1 expression) vectors in *KLC1*$^{-/-}$ neurons. Transfected neurons were stained with KLC1 antibody to confirm the recovery of KLC1 expression (Fig. 7B). The overexpression of KLC1 in neurons depleted of endogenous KLC1 restores the movement of CB1R vesicles by increasing anterograde and retrograde vesicle proportion to *KLC1*$^{+/+}$ levels and by reducing the proportion of stationary vesicles (Fig. 7D).”

Figure 7

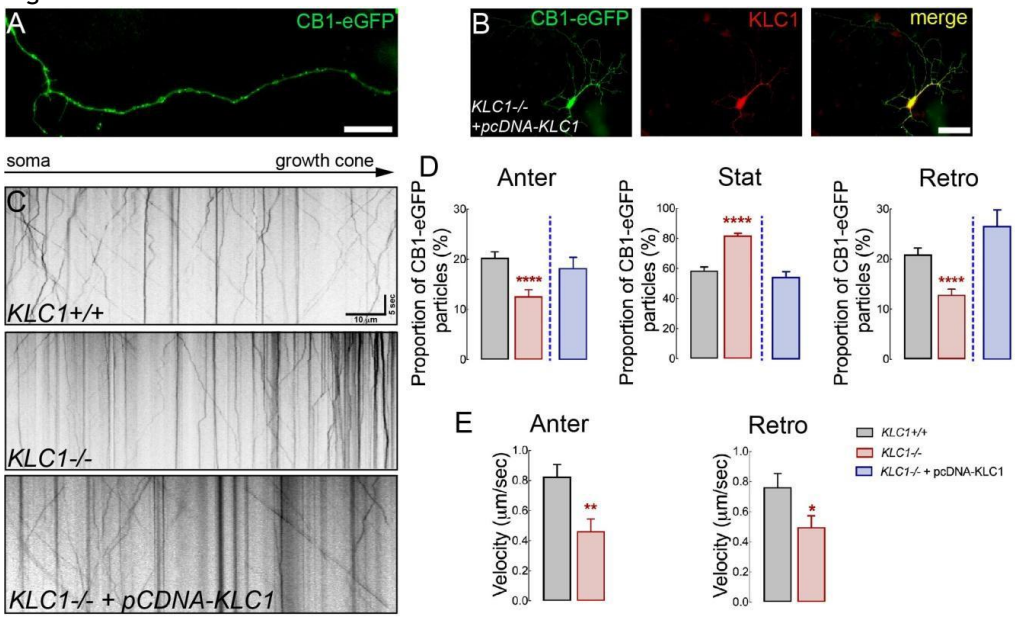

Figure 7. CB1R axonal transport is impaired in *KLC1*$^{-/-}$. (A) Representative epifluorescence images obtained from a live-cell movie of 7-8 DIV hippocampal neurons transfected with CB1R-eGFP. (B) Hippocampal neuron co-transfected with CB1R-eGFP plus pcDNA-KLC1 and immunostained for GFP and KLC1. (C) Kymographs of CB1R-eGFP transfected neurons obtained from live-cell imaging of *KLC1*$^{+/+}$, *KLC1*$^{-/-}$, and *KLC1*$^{-/-}$+pcDNA-KLC1 hippocampal cultures. (D) Anterograde, stationary and retrograde proportion of CB1R-eGFP vesicles, and (E) average velocities for anterograde and

retrograde CB1R-eGFP vesicles. Data is expressed as means ± s.e.m. *Student's t*-test, n = 52 KLC1$^{+/+}$, 43 *KLC1*$^{-/-}$, 34 *KLC1*$^{-/-}$+pcDNA-KLC1 neurons from 3 independent experiments. Scale bar: 20 µm (A). **p<0.001, ***p<0.0001.

- Time lapse imaging of growth cone to assess their dynamism in KLC-/- vs +/+ mice necessary.

As the reviewer suggested, we set up the conditions to follow the dynamics of growth cones in *KLC1*+/+ and *KLC1*-/- neurons in culture by time lapse after the transfection with pCMV-lifeAct-Ruby. LifeAct preferentially binds to filamentous actin (F-actin) and thereby allow a direct visualization of F-actin at the growth cone. We obtain two nice sets of measurements from this experiment that showed no changes in growth cone dynamics in *KLC1*+/+ and *KLC1*-/- within the time frame of analysis. It is possible that longer time point of cone dynamic registration or the challenge with agonist or antagonist would reveal differences; however, we were unable to perform it in this revision time frame. The technique and results obtained are presented bellow but were excluded from main manuscript.

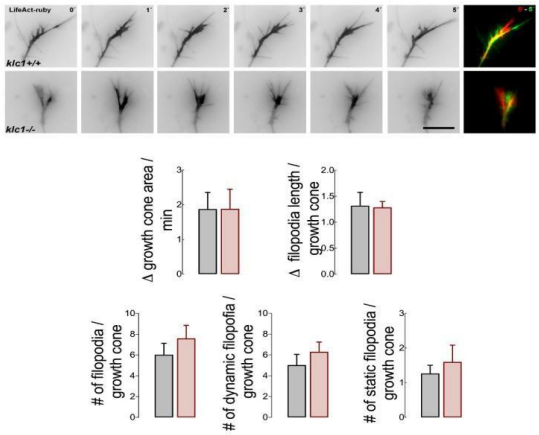

Figure. Growth cone dynamics followed by filamentous actin detection. (A) Representative time lapse images of axonal growth cones obtained from *KLC1*$^{+/+}$ and *KLC1*$^{-/-}$ cortical neurons transfected with pCMV-lifeAct-Ruby. Images were acquired at 5 s intervals for 5 min. (B) Quantification of dynamic parameter between last (5 min) and first frame (0 min). Data is expressed as means ± s.e.m. Scale bar: 5 µm.

- Kinesin is not a specific molecular motor. I recommend analyzing at least one more cargo to demonstrate how specific the overall finding is in these axons.

This is a very interesting observation made by the reviewer that was already assessed in previous experiments by our group. We have now included the following statement in discussion for clarification:

"The specificity of KLC1-dependent cargos was previously assessed showing selective impairments for another cargo such as the Amyloid Precursor Protein vesicle while mitochondria axonal transport was not affected (Falzone et al JON 2009), suggesting that not overall microtubule dependent dynamics are impaired when KLC1 is deleted from neurons."

- Figure 9: a more detailed analysis is needed here. At least, a regular sholl analysis would help to support the conclusion that only axonal elongation is affected. How is the effect on axonal elongation fitting together with the changed axonal bundles in the beginning?

We have now expanded and improved our analysis to show the properties of axonal branching and the dendritic arborization parameters in neurons from *KLC1*$^{+/+}$ and *KLC1*$^{-/-}$. Branching was measured in all axonal projections from control and treated (ACEA) conditions for *KLC1*$^{+/+}$ and *KLC1*$^{-/-}$ neurons showing no changes in ramification of axons. In addition, Sholl analysis also showed similar dendritic arborization between *KLC1*$^{+/+}$ and *KLC1*$^{-/-}$. This was included in now Figure 10 C, D as follow:

"To test whether KLC1 is relevant for CB1R-dependent axonal elongation, we analyzed the axonal length of cortical neurons in culture under DMSO or the CB1R agonist ACEA. Interestingly, axonal extension evaluated in neurons at DIV 4 were similar in both *KLC1*$^{+/+}$ and *KLC1*$^{-/-}$ treated with

DMSO, suggesting a normal intrinsic axonal growth process for *KLC1*$^{-/-}$ neurons without the stimulation of external guiding clues (Fig. 10A, B). The stimulation of CB1R with ACEA (300 nM) induced a significant increase (40%) in axonal elongation compared with DMSO in *KLC1*$^{+/+}$ neurons (Fig. 10A, B), reinforcing the knowledge that eCB promote axonal extension. However, *KLC1*$^{-/-}$ neurons were unable to respond to the treatment with ACEA showing similar axonal length than *KLC1*$^{-/-}$ in DMSO conditions (Fig. 10A, B). Axonal branching and dendritic arborization using Sholl analysis was measured in *KLC1*$^{+/+}$, and *KLC1*$^{-/-}$ after DMSO or ACEA treatment without revealing significant morphological changes (Fig. 10C, D). Together, we showed that CB1R activity involves a regulation that drives the axonal elongation process. Moreover, *KLC1*$^{-/-}$ neurons display a normal intrinsic program of axonal extension, however, are unable to respond to external clues that further promote axonal elongation through the specific stimulation of CB1R"

Figure 10

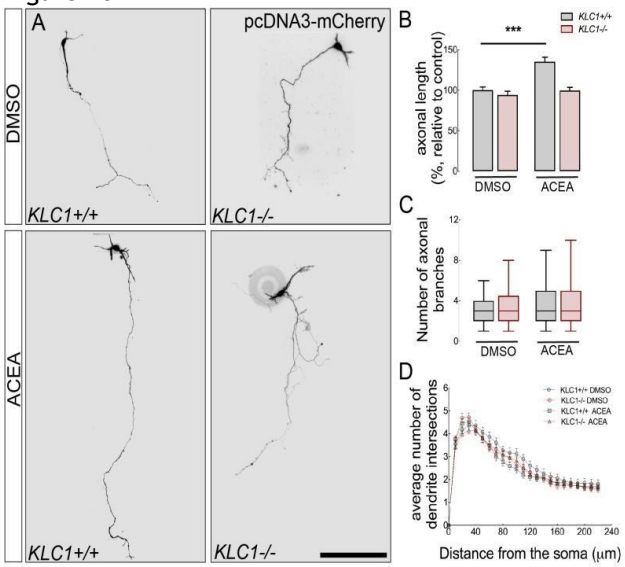

Figure 10. KLC1$^{-/-}$ **neurons are unresponsive to CB1R-mediated axonal elongation.** (A) Representative epifluorescence images of *KLC1*$^{+/+}$ and *KLC1*$^{-/-}$ primary cortical neurons transfected with pcDNA3-Cherry and treated for 72 hours with DMSO or ACEA (300 mM). (B). Axonal length quantified in pcDNA-Cherry transfected neurons. Data is expressed as means ± s.e.m. Two way-ANOVA; neurons for *KLC1*$^{+/+}$: n = 80 (DMSO), 64 (ACEA); *KLC1*$^{-/-}$: n = 61 (DMSO), 61 (ACEA), from 3 independent experiments. (C) Quantification of the number of primary axonal branches. Data is expressed as median ± 25/75 percentiles. (D) Sholl analysis to quantify the average number of dendrite intersections. Data is expressed as means ± s.e.m. *KLC1*$^{+/+}$: n = 84 (DMSO), 66 (ACEA); *KLC1*$^{-/-}$: n = 83 (DMSO), 94 (ACEA) neurons, from 3 independent experiments. Scale bar: 200 μm. ***p < 0.001.

- Has the fasciculation defects something to do with membrane adhesion defects?
This is a very interesting question that our work did not specifically tackle. Cell Adhesion Molecules are key for the development and guidance of axonal tracks. Impairments in the function of CAMs have been associated with axonal pathfinding defects. We have not observed significant changes in L1-NCAM staining between *KLC1*+/+ and *KLC1*-/-, and the dynamics of L1-NCAM seems to be independent of Kinesin-1 axonal transport (Peretti D. et al JCS 2000). However, this not exclude that other cell adhesion molecules (NCAM140 and NCAM180) that depends on kinesin-1 for their Golgi derived delivery into axons might be affected in KLC1-KO mice (Wobst H et al JCS 2015).

- Statistics section is missing in Methods. Why did the authors use a t-test and not a non- parametric test? Are the data tested for normal distribution? Please state the number of experiments throughout the manuscript, not only the single axons.

We apologize for the missing description of the statistical methods used. It is now included in materials and methods and below. Figure legends are also now improved to show clearly the statistics used, n of experiments and significances.

“Statistical Analysis

Statistical differences between conditions were assessed using GraphPad Prism 8.2.1., MATLAB and R core team (2017). The normal distribution of the samples was assessed prior to analysis of significance. Values are expressed as means ± standard error of the mean (s.e.m.) or median ± 25/75 percentiles for non parametric data for the indicated number of independent experiments or corresponding particles (n). The experimental setting, the n, and the number of independent experiments are described in figure legends. No data was excluded from analysis. Images for analysis of intensity, quantification of axonal tracks from movies, or in Sholl analysis were double-coded so experimenter was blind to genotype or treatment. A two-tailed *Student’s t*-test was used to compare differences between groups. Two-way ANOVA was performed to identify the interaction between two independent variables and analysis was followed by a *Bonferroni* post-test. *Kolmogorov-Smirnov* test was used to compare frequencies distributions of fascicles diameter, segmental velocities and axon diameters. Differences that resulted in $p < 0.05$ were considered to be significant.”

Minor points:
- Figure 1: section thickness would help to better judge the phenotype.

Included as follow: “Representative epifluorescence images of 50 µm coronal brain sections”…

- Line 128: Figure 1G does not exist.

Corrected

- Line 140: “specific role”: I would tone this down a bit.

Was toned down as follow: “Altogether, our results suggested that KLC1 might be involved in the development of CFA and TCA connectivity.”

- Line 141: remove typos.

Corrected

- Line 150: reference needed here!.

Included

Second decision letter

MS ID#: DEVELOP/2019/184069

MS TITLE: Kinesin-1-mediated axonal transport of CB1 receptors is required for cannabinoid-dependent axonal growth and guidance

AUTHORS: Trinidad Maria Saez, Ivan Fernandez Besssone, Maria Sol Rodriguez, Matias Alloatti, Maria Gabriela Otero, Lucas Cromberg, Victorio Pozo Devoto, Gonzalo Oubina, Lucas Sosa, Mariano G Buffone, Diego Gelman, and Tomas Falzone
ARTICLE TYPE: Research Article

I am happy to tell you that your manuscript has been accepted for publication in Development, pending our standard ethics checks.

Reviewer 1

Advance summary and potential significance to field

Authors have adequately addressed all comments and criticisms raised on the first version, and the manuscript has improved significantly

Comments for the author

None

Reviewer 2

Advance summary and potential significance to field

My previous concerns are now addressed and I the authors performed an adequate revision. I see the manuscript suitable for publication now!

Comments for the author

The authors have done a number of experiments and substantially improved the manuscript.